Institute of Paper Science and Technology
Atlanta, Georgia

IPST TECHNICAL PAPER SERIES

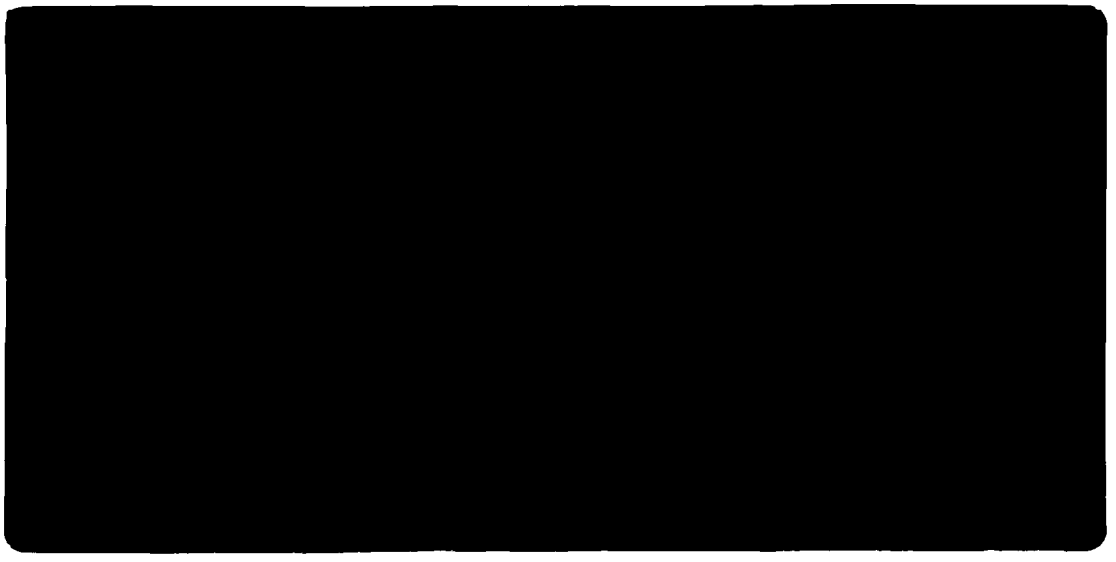

NUMBER 508

CFD SIMULATIONS OF THE INTERACTION BETWEEN AIR JETS AND DIFFERENT CHAR BED SHAPES IN RECOVERY FURNACES

W. YANG, R.R. HORTON, AND T.N. ADAMS

JANUARY 1994

CFD Simulations of the Interaction Between Air Jets and Different Char Bed Shapes in Recovery Furnaces

W. Yang, R.R. Horton, and T.N. Adams

Submitted to
Tappi Journal

ABSTRACT

This paper presents the results of investigations of the interaction between air jets and the char bed in a black liquor recovery furnace. A section of the lower furnace region is examined using Computational Fluid Dynamics (CFD). Three char bed shapes and two model geometries are examined. Air flow patterns, shear stress, and mass transfer coefficient on the bed surface are calculated. The results show that the primary air jets have strong impact on the perimeter of the char bed. The profiles for the primary jets depend on the char bed slopes. A steep slope results in fast dissipation and short air jets. Interaction between secondary air jets and the char bed occurs only if the char bed reaches the secondary air level, and the interaction is mainly determined by the air port-to-surface spacing. The shear stress and mass transfer coefficient distributions suggest that a stable char bed for the given air flow patterns may have a slope of about 1:2 and a height just below the secondary air level. This agrees with field observations.

INTRODUCTION

Char bed combustion in black liquor recovery furnaces is an important part of furnace operations. The char bed should have an adequate char burning rate, a high sulfate reduction efficiency, and a stable shape that minimizes particle entrainment and carryover. Interaction of air jets on bed surface is a major factor that affects the combustion processes in the char bed because under normal operation conditions, char bed burning is essentially limited by the rate of oxygen supply (1). Since the oxygen supply depends on air flow patterns, the air jets have significant influence on char combustion and char bed shape. In turn, the shape of the char bed affects air flow patterns by deflecting air jets that impinge on the bed surface (2, 3). A good understanding of the interaction between the air jets and the char bed can help design efficient furnaces and optimize operation conditions.

Computational Fluid Dynamics (CFD) is an efficient method for studying gas flow and combustion processes in recovery furnaces. Applications of the CFD technique to recovery furnace simulations have produced useful results for air flow patterns (4 - 13), temperature and concentration distributions (6 - 8, 14), trajectories of black liquor particles (6, 16), and particle entrainment (16). Simulations of black liquor combustion in a char bed involves chemical reactions, mass transfer, and heat transfer on the bed surface (7, 15). Since the shape of the boundary is not known beforehand, assumed char bed shapes have been used in simulations (2, 3, 7). This may introduce errors in the results; however, such studies can provide information for feasible char bed shapes and may eventually lead to the prediction of char bed shapes from operation conditions.

A limiting factor for CFD simulations of recovery furnaces is that the requirement for computer memory and CPU time can easily exceed practical limits. The overall size of a typical furnace is large relative to its small features, such as air ports. Thus, a CFD furnace model requires large numbers of computational cells to resolve details in a full model. The complexity of the processes in a furnace makes the simulations even more memory and time intensive. An efficient way to reduce the size of a CFD model without losing details is to

simulate a small zone of interest by isolating the zone from the rest of the furnace with suitable boundary conditions. A symmetry plane is the most frequently used boundary type for simplifying recovery furnace simulations (5, 8, 14). This technique is especially helpful for char bed simulations. With reduced simulation zones, smaller computational cells can be used to describe the furnace structure and char bed shape more accurately.

Application of CFD technique to char bed simulations is a complicated problem which involves chemical reactions, transport processes, fluid dynamics, and numerical methods. This paper represents a part of an ongoing study on char bed simulations. In previous articles (2, 3), the effects of grid type and selection of boundary geometry on simulation results were examined. In this work, the interaction between air jets and char beds is studied using CFD simulations in the lower region of a furnace. Gas flow patterns, shear stress and mass transfer coefficient on the bed surface are calculated for different char bed shapes. Feasible char bed shapes are qualitatively described from the distribution patterns of the shear stress and the mass transfer coefficient. In this and the previous studies, CFD simulations are restricted to a slice of the lower furnace region in order to resolve details of the flow patterns with limited computational ability. In a future study, simulations will be carried out in a larger region with a coarser grid to examine the interaction between the char bed and air jets from adjacent furnace walls.

In the following sections, the char bed models will be described, then simulation results for air flow patterns and air jet-char bed interaction will be presented, followed by conclusions from this study.

DESCRIPTION OF CHAR BED MODELS

Attention is focused on the lower furnace region where air jet-char bed interaction takes place. The horizontal cross-section of the full furnace is a 10 m square. The air ports are symmetrically arranged on furnace walls. The primary air ports are 0.05 m wide and 0.3 m high, with an elevation of 0.05 m and a spacing of 0.3 m. The secondary air ports are

0.15 m wide and 0.5 m high, with an elevation of 1.5 m and a spacing of 1.5 m. The inlet air velocities are assumed to be uniform across individual air ports. The primary air velocity is 50 m/s in a 10° downward angle, the secondary air velocity is 80 m/s in the horizontal direction. Heat transfer and chemical reactions are not included in the present study, so an isothermal condition is assumed and the physical properties of air at 1000 °C are used.

To examine effects of char bed shape on the air jet-char bed interaction, three simplified char bed shapes are used in the simulations. All the char beds have straight slopes and flat tops. The char bed surfaces start to rise at 0.15 m from the wall with 1:1, 1:2, or 1:4 slope, and then level off either at 1.775 m above the baseline or at 3.7 m from the wall. The 1:4 slope results in a bed that is only half the height of the beds of 1:1 and 1:2 slopes.

To resolve details of the gas flow patterns, a large number of small computational cells must be used. Therefore, only a small section of the lower furnace region is included in the models. Two arrangements of symmetry planes are considered in this work: a slab geometry and a wedge geometry. The slab models include a uniform width slice of the char bed isolated from the furnace by two parallel and one central symmetry planes and an upper isobaric boundary. The thickness of the slab is 0.75 m, including 2½ primary air ports and ½ secondary air port, as shown in Figure 1. Part of the upper boundary of the computational region is sloped to achieve efficient node distributions. The effect of a sloped boundary on gas flow field is negligible since gas velocity is very low near the sloped boundary. The slab models are equivalent to furnaces with air ports on two infinitely long opposing walls. In this case, the air jets from the other two walls of a four-wall furnace have negligible effect.

In the wedge geometry, one of the side symmetry planes is slightly angled so that the symmetry planes on both sides meet at the furnace center, as shown in Figure 2. This is a rough approximation of a symmetrical furnace with air ports on four walls. As the air jets travel from the wall to the furnace center, the cross-sectional area reduces gradually as if the jets were pushed by air jets from the adjacent walls. With the same inlet air flow rate, the average vertical velocity of the wedge models is twice that of the slab models. Technically, a

wedge model corresponds more closely to a nearly circular furnace with uniformly distributed air ports around the wall. Air jets in the middle of a symmetrical square furnace correspond approximately to a situation between the slab and the wedge models.

The simulations were carried out with FLUENT Version 4.11 (Fluent Inc.), a CFD software based on the finite difference method (17). Body-fitted-coordinate (BFC) grids were used so that the char bed slopes could be represented by smooth boundary conditions (18). In comparison with Cartesian coordinate grids, which must use stairsteps to represent sloped boundaries, BFC grids offer improved accuracy, especially for shear stress and mass transfer coefficient on the sloped surface, and faster convergence speed (3).

All the models in this study have the same number of computational cells (57×52×27× = 80,028). Simulations with nearly 150,000 cells show that the solutions are nearly grid-independent. Slight grid dependence does not affect the utility of the results, as the main interest is in the differences between the models that are more significant than the effects of the grid. The κ-ε turbulence model was used for all computations and the software was run on an IBM RISC/6000 computer, model 550.

RESULTS AND DISCUSSION

Effect of Bed Shape on Gas Flows

In the 1:1 and 1:2 slope models, the char beds reached the secondary air level. Strong interaction between the air jets and the char beds is expected for these models. Figure 3 shows velocity distribution patterns near the boundaries for all cases. An apparent difference between the slab and the wedge models is that the secondary air jets turn upward earlier in the wedge models than in the slab models. However, the primary air jets are only slightly affected by the wedge shape. More discussion about the effects of the wedge shape can be found in a previous paper (2).

In all the models, the primary air jets impinge on the char bed surfaces within a short distance. The slopes of the char beds determine impinging angles of the air jets, and strongly affect the flow patterns. In the case of a 1:1 steep slope, which corresponds to a large impinging angle, the primary jets are deflected abruptly upon impinging on the bed surface. Strong interaction between neighboring jets causes the primaries to dissipate in a short distance. As the slope decreases, the primary jets extend greater distances into the furnace.

A char bed influences the secondary air jets when the height of the bed reaches the secondary air level. For the beds with the same height (1:1 and 1:2 slopes), the 1:1 slope bed is closer to the secondary air port so it has a stronger influence. In the case of a 1:1 slope, (Figures 3(a) and (b)), the secondary jets undergo sudden compression in the y direction and expansion in the z direction. This process enhances dissipation and reduces jet velocity. A high pressure region that is formed at the point of impingement forces the primary air to deviate from its original flow direction. In the case of a 1:2 slope, the slab and the wedge models show remarkably different air jet-char bed interaction. In the slab model, the secondary jet extends horizontally and impinges on the top of the char bed. In the wedge model the secondary air jet turns upward before it contacts the bed surface, resulting in little air jet-char bed interaction. If a char bed is below the secondary air level, it has little apparent effect on the secondary air flows in either the slab or the wedge model (Figure 3(e) and (f)).

Figures 4 and 5 compare average vertical velocities at the upper boundaries. All the models predict a high velocity central core, which is typical for symmetrical air distributions. The wedge models predict higher velocities at the furnace center than the slab models because they have smaller cross-sectional areas and the air jets are forced to turn upward sooner by the converging side boundaries. Impingement of the air jet on the char bed enhances dissipation, as is shown by the decrease of the velocities with increasing char bed slopes in the slab models. The situation is similar for the wedge models, except that the case with a 1:2 slope has a lower velocity at the furnace center than the other cases because a high pressure region above the top of the bed forces the secondary jet to turn upward sooner.

Impacts of Air Jets on Char Bed Surfaces

Impingement of an air jet on a char bed affects the mass and heat transfer processes and redistribution of char particles on the bed surface. All of these processes are related to the shear stress on the bed surface. Figure 6 shows plan views of the shear stress distributions. The bright areas highlight strong interactions between the air jets and the char beds. Generally, the impact of an impinging jet on a surface depends on the air port-to-surface distance and angle of impingement. For the primary air jets, the air port-to-surface distance does not vary significantly with the slope of the char bed, however, the angle of impingement varies with the slope. As the slope of the char bed decreases, the angle of impingement decreases and the primary air jets extend further along the bed surface. As a result, the areas of large shear stress increase in the x direction.

The secondary air ports are a greater distance to the char bed, thus, the effect of air port-to-surface distance is more significant than that of the angle of impingement. Comparing Figures 6(a) and (c), the maximum shear stress due to the secondary air jets decreases from 3.92 Pa to 1.44 Pa when the air port-to-surface distance increases from 1.92 m to 3.7 m. With the same change in distance, the wedge models show an even more remarkable decrease in the shear stress because the secondary air jet no longer impinges on the char bed with the 3.7 m distance. In the case of a 1:4 slope, since the char beds are well below the secondary air level the secondary air jets have no contribution to the shear stress distributions, as can be seen in Figures 6(e) and (f).

The average shear stress distributions are plotted in Figures 7 and 8. The shear stresses due to the primary jets have comparable maximum values that are not very sensitive to the slopes of the char bed. However, the distribution profiles are strongly affected by the slopes. The steeper the slope, the faster the shear stress decreases. In the case of a 1:1 slope, the secondary air jets produce spots of very large shear stress at the top of the char beds. This may be partly due to the angled edges of the flat bed tops. If the char bed surfaces had rounded edges, the shear stress distributions would not change so abruptly.

In the present simulations, the char bed surface is assumed to be smooth. This causes the shear stress to be underestimated because practical char bed surfaces are rough. Roughness parameters would have to be specified for more realistic simulations. The roughness parameter affects the magnitude of the shear stress significantly. However, the distribution patterns would probably not be affected.

Mass transfer on the bed surface plays a major role in determining the rate of char combustion. Mass transfer coefficient can be estimated from the shear stress and velocity using the Chilton-Colburn analogy (19):

$$St_m Sc^{\frac{2}{3}} = \frac{C_f}{2} \tag{1}$$

where $St_m = k/u_p$ is the Stanton number for mass transfer; k is the mass transfer coefficient; u_p is velocity near the surface; Sc is the Schmidt number of the gas (≈ 0.7); C_f is the friction factor, which can be calculated from the shear stress, τ_w, and the velocity by:

$$C_f = \frac{\tau_w}{\frac{1}{2}\rho u_p^2} \tag{2}$$

Combining Equations (1) and (2) to give

$$k = \frac{\tau_w}{\rho u_p} Sc^{-\frac{2}{3}} \tag{3}$$

The above equations have been confirmed to agree with experimental results of black liquor combustion (15). Average mass transfer coefficient for the present models are shown in Figures 9 and 10. As expected, the profiles of the mass transfer coefficient have similar patterns as the shear stress profiles. The distributions of the shear stress and the mass transfer coefficient may provide clues to realistic char bed shapes.

Char Bed Shapes

The shapes of char beds are the results of many physical and chemical processes. The arrival of char particles is mainly determined by black liquor spray patterns and is affected by gas flow patterns. The combustion and redistribution of char particles on the char bed surface depend on air flow patterns, as well as the shape of the bed. Mechanical processes, such as collapse of an undercut bed, will also contribute to the formation of a bed shape.

The air jet-char bed interaction is an important part of char bed formation processes. At typical furnace operation temperatures (> 1000 °C), char combustion by O_2 is essentially controlled by mass transfer. In the areas of air jet impingement, combustion takes place faster than in other areas due to higher O_2 concentration and larger mass transfer coefficient. In the areas where the air jets cannot reach directly, O_2 supply may be deficient, and char gasification by CO_2 and H_2O may become important. The gasification reactions are slower than the combustion by O_2, and these endothermic reactions may reduce the local surface temperature and slow down the reaction rates.

In the cases of 1:1 and 1:4 slopes, the mass transfer coefficient distributions are similar for the slab and the wedge geometries. The char beds with a 1:1 slope represent one extreme where the primary and secondary air jets impinge hard on the bed surfaces. This can result in very nonuniform combustion rate distributions. Very fast combustion can be expected near the bottom and the top surfaces of the char beds. If the char arrival pattern does not cause excessive accumulations in these areas, then the top surface will be burnt off and the bottom surface will be undercut. Consequently, the char bed would collapse, becoming less steep. In contrast, the char combustion rate varies less abruptly on the bed with a 1:4 slope. Faster combustion occurs near the base of the bed where the primary jets impinge on it. As the air flows toward the center of the furnace, O_2 concentration and mass transfer coefficient decrease gradually. Combustion rate at the furnace center can be expected to be lower than that near the walls. This implies that the char bed would have the tendency to grow higher at the center.

The slab and the wedge models with a 1:2 slope show different combustion patterns. The effects of the primary air jets are similar: increasing combustion rate near the base of the bed. The slope of the bed is already small, thus collapse is not likely to occur. The straight slope, however, may change into a complex curved shape. In the slab model, impingement of the secondary jet on the top of the bed creates a fast burning area. This may prevent the char bed from growing higher or steeper since the combustion rate increases quickly with the growth of the bed. Significant decrease of the bed size is not likely either since that would lead to a situation similar to the case of a 1:4 slope. A stable bed shape may have approximately a 1:2 slope with the top at the secondary air jet level. In the wedge model with a 1:2 slope, the secondary air jet does not extend horizontally far enough to reach the char bed. Char combustion rate at the top of the bed is expected to be smaller than that in the corresponding slab model. Therefore, the wedge model would predict a higher char bed than the slab model.

Combustion is only one aspect of the char bed formation process. Accurate prediction of the char bed shape is not possible unless char arrival and mechanical char redistribution processes are also considered. An actual char bed shape is determined by the balance of overall char arrival and removal.

CONCLUSIONS

Interaction between air jets and black liquor char beds has been studied using CFD simulations. Three char bed shapes and two model geometries have been examined. The following conclusions may be drawn from the results.

1. There is strong interaction between primary air jets and char beds. The flow patterns of the jets depend on the slopes of the char beds. The smaller the slope, the further the jets extend, but the weaker the initial impact on the bed.

2. The interaction between secondary air jets and char beds depends on the air port-

to-surface distance. The smaller the distance the stronger the interaction. There is minimal interaction between secondary air jets and a char bed if the char bed is below the secondary air level.

3. Air jet impingements produce areas of high mass transfer coefficients. The distribution of the mass transfer coefficients is very sensitive to the char bed shape. With the assumed air system, a stable char bed may have a slope between 1:4 and 1:1, and a height reaching the secondary air level.

ACKNOWLEDGMENT

This work was supported by the U.S. DOE under contract No. DE-FG02-90CE40936, and IPST member company funding.

REFERENCES

1. Grace, T. M., Lien, S. J., and Brown, C. A., "Char Bed Burning - Laboratory Studies," *Proc. Int'l Chem. Recovery Conf.*, p. 539, 1992.

2. Yang, W., Horton, R. R., and Adams, T. N., "A Comparison of CFD Simulations of Recovery Boiler Char Beds with 2-D and 3-D Geometries," IPST Technical Paper series #483, 1993.

3. Yang, W., Horton, R. R., and Adams, T. N., "CFD Simulations of Recovery Boiler Char Beds with Step and Smooth Surfaces," IPST Technical Paper Series, #478, 1993.

4. Chapman, P. J. and Jones, A. K., "Recovery Boiler Secondary Air System Development Using Experimental and Computational Fluid Dynamics," *Proc. TAPPI Eng. Conf.*, p. 193, 1990.

5. Jones, A. K. and Grace T. M., "A Comparison of Computational and Experimental Methods for Determining the Gas Flow Patterns in the Kraft Recovery Boiler," *Proc. TAPPI Eng. Conf.*, p. 3, 1988.

6. Chapman, P. J. and Jones, A. K., "Recovery Furnace Combustion Modeling Using Computational Fluid Dynamics," *Proc. Int'l Chem. Recovery Conf.*, p. 71, 1992.

7. Sumnicht, D. W., "A Computer Model of a Kraft Char Bed," Ph.D. Thesis, IPC, April, 1989.

8. Vakkilainen, E. K., Adams, T. N., and Horton, R. R., "The Effect of Recovery Furnace Bullnose Designs on Upper Furnace Flow and Temperature Profiles," *Proc. Int'l Chem. Recovery Conf.*, p. 101, 1992.

9. Siiskonen, P., Karvinen, R., Hyoty, P., Migaj, V. K., and Morgoun, A. V., "Combined Physical and Numerical Study of a Multilevel Air System," *Proc. Int'l Chem. Recovery Conf.*, p. 57, 1992.

10. Salcudean, M., Nowak, P., and Abdullah, Z., "Mathematical Modeling of Recovery Furnaces," *Proc. Int'l Chem. Recovery Conf.*, p. 197, 1992.

11. Abdullah, Z., Nowak, P., Salcudean, M., and Gartshore, I. S., "Investigation of Interlaced and Opposed Jet Arrangements for Recovery Furnaces," *Proc. TAPPI Eng. Conf.*, p. 103, 1992.

12. Quick, J. W., Gartshore, I. S., and Salcudean, M., "Interaction of Opposing Jets with Special Relevance to Recovery Furnaces," *Proc. TAPPI Eng. Conf.*, p. 123, 1992.

13. Adams, T. N. and Horton, R. R., "The Effects of Black Liquor Spray on Gas Phase

Flows in a Recovery Boiler," *Proc. TAPPI Eng. Conf.*, p. 81, 1992.

14. Karvinen, R., Hyoty, P., and Siiskonen, P., "The Effect of Dry Solids Contents on Recovery Boiler Furnace Behavior," *Tappi J.* **74**(12), 171(1991).

15. Sutinen, J. E. and Karvinen, R., "Numerical Modeling of Char Bed Phenomena," *Proc. Int'l Chem. Recovery Conf.*, p. 79, 1992.

16. Horton, R. R., Grace, T. M., and Adams, T. N., "The Effects of Black Liquor Spray Parameters on Combustion Behavior in Recovery Furnace Simulations," *Proc. Int'l Chem. Recovery Conf.*, p. 85, 1992.

17. FLUENT User's Guide, Ver. 4.0, Fluent Inc., December 1991.

18. PreBFC User's Guide, Ver. 4.0, Fluent Inc., December 1991.

19. Incropera, F. P. and De Witt, D. P., *Fundamentals of Heat and Mass Transfer*, 2nd ed., John Willey & Sons, New York, 1985.

20. Launder, B. E. and Spalding, D. B., *The Numerical Computation of Turbulent Flows*, Imperial College of Science and Technology, London, 1973.

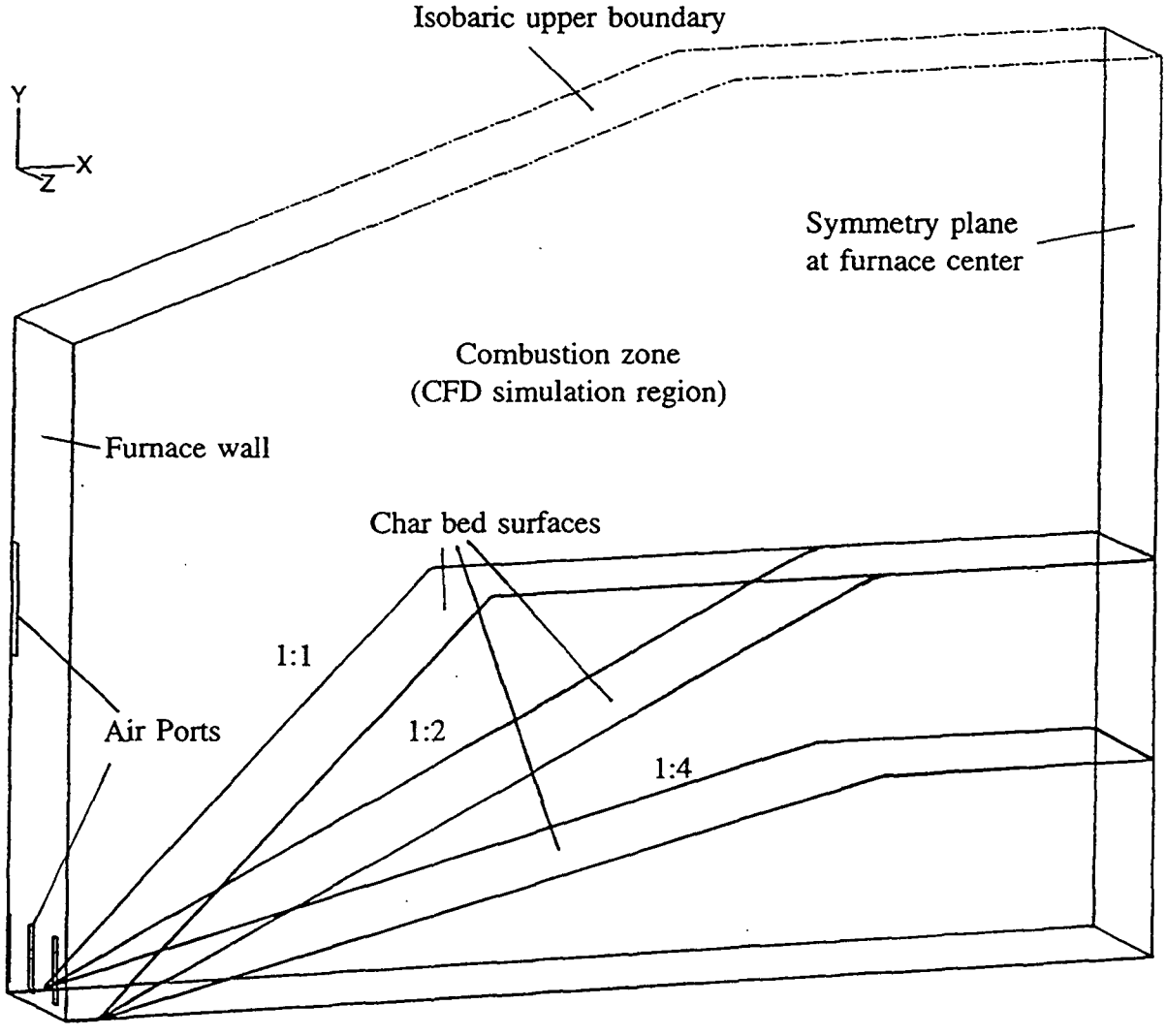

Figure 1. Geometries of slab char bed models with 1:1, 1:2, and 1:4 slopes.

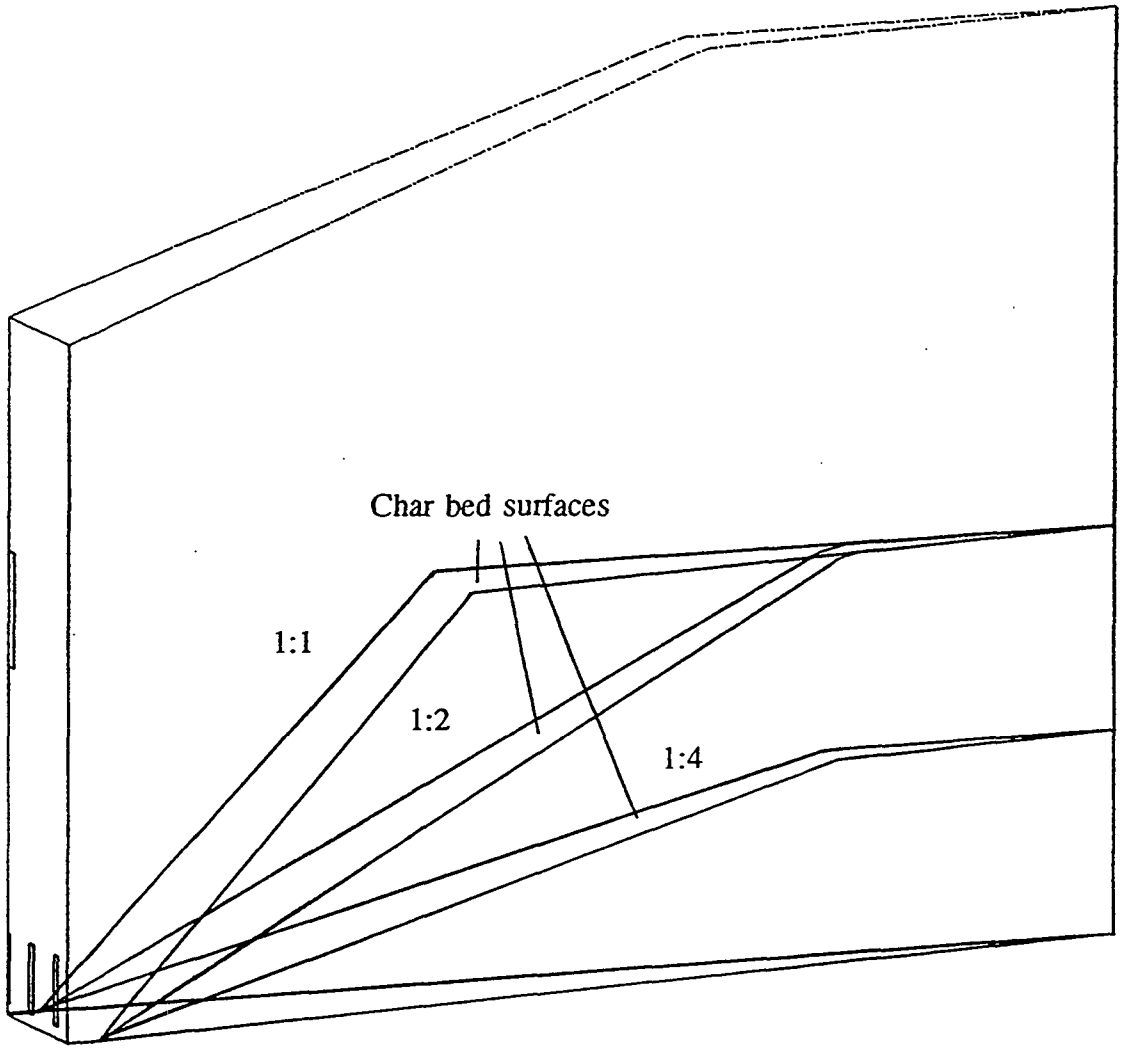

Figure 2. Geometries of wedge char bed models with 1:1, 1:2, and 1:4 slopes.

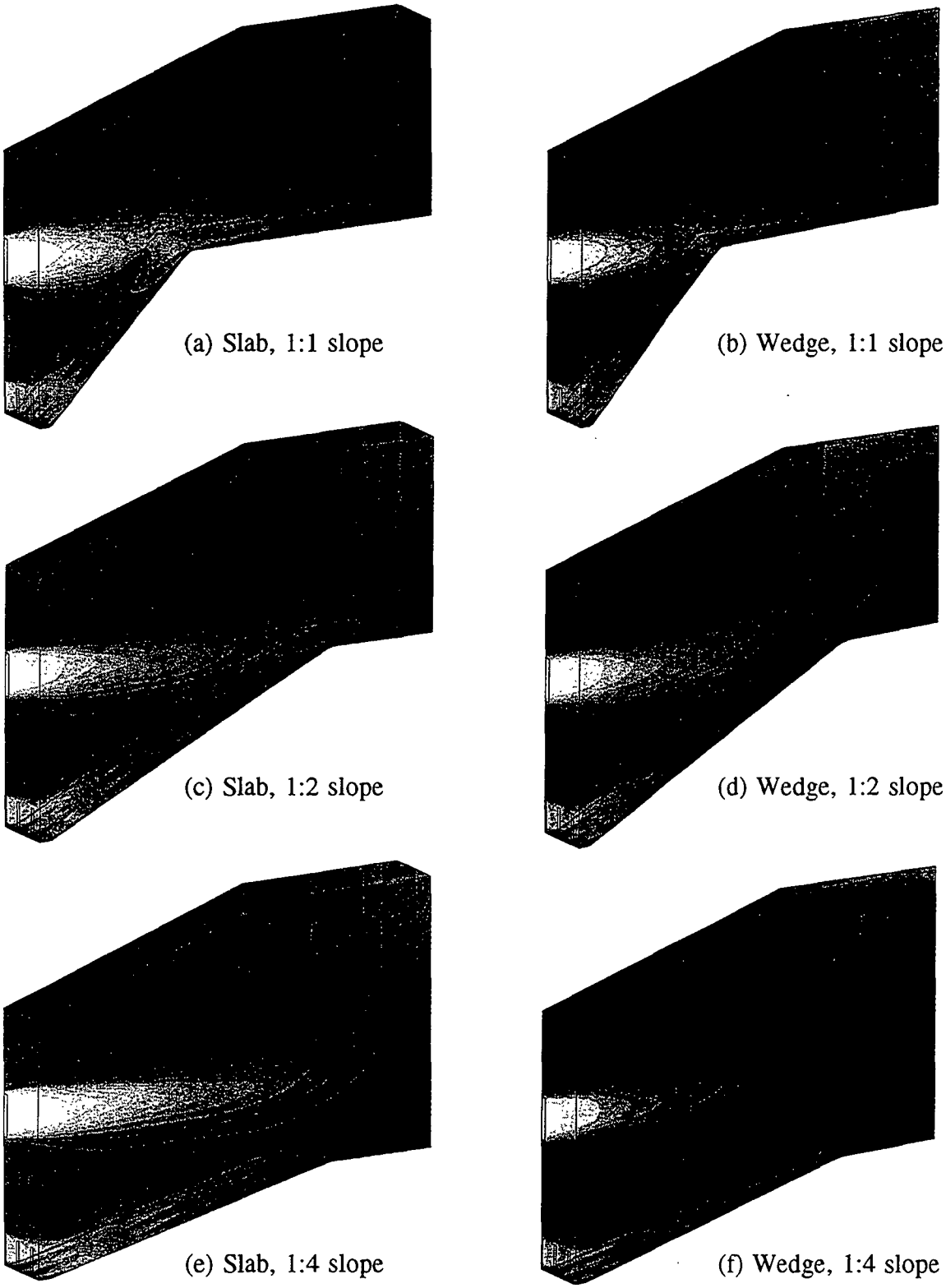

Figure 3. Flow patterns on boundary surfaces in different models.
Gray scale = 0 - 80 m/s (dark - bright).

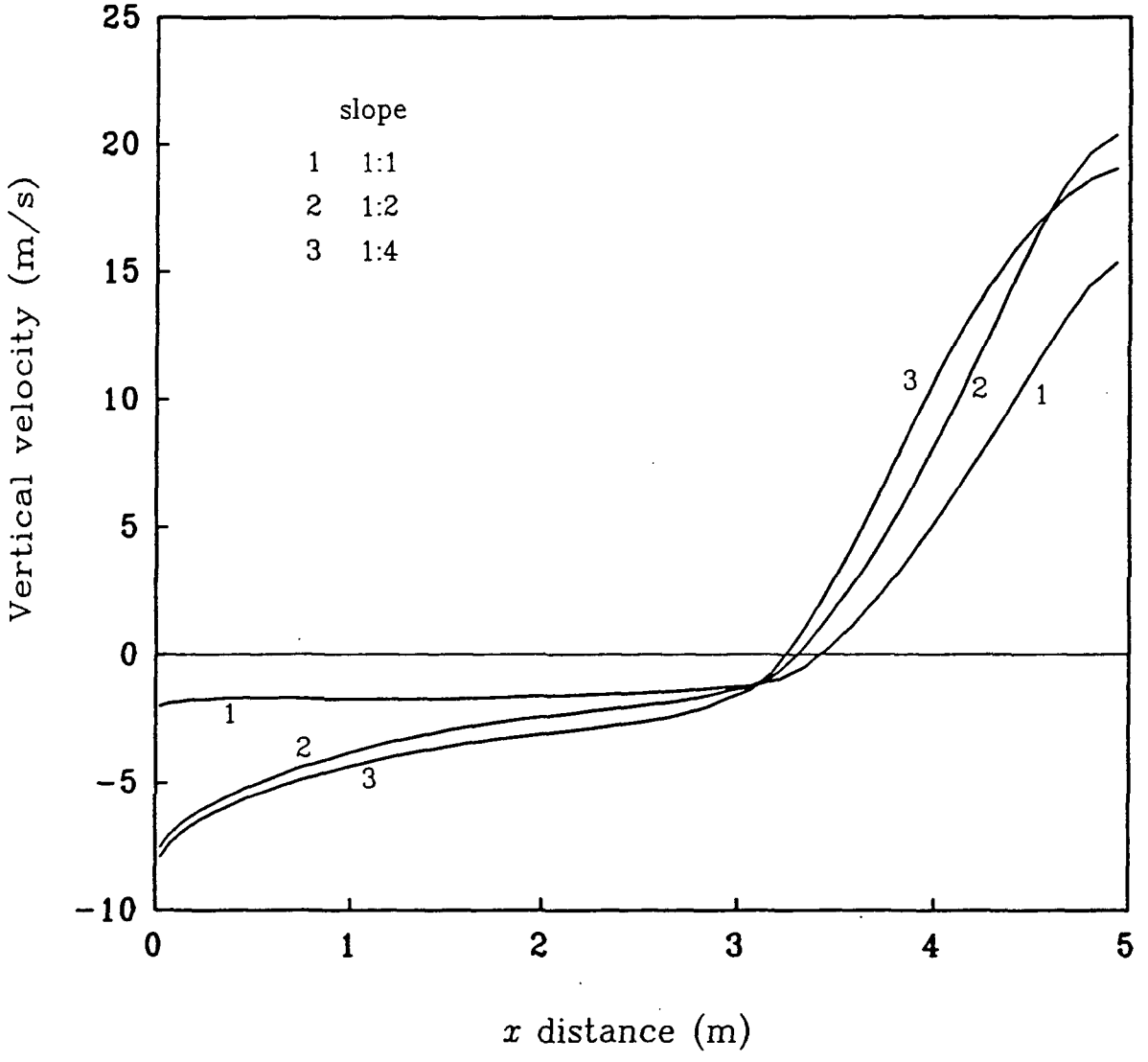

Figure 4. Average vertical velocity distributions at the upper boundaries in the slab models.

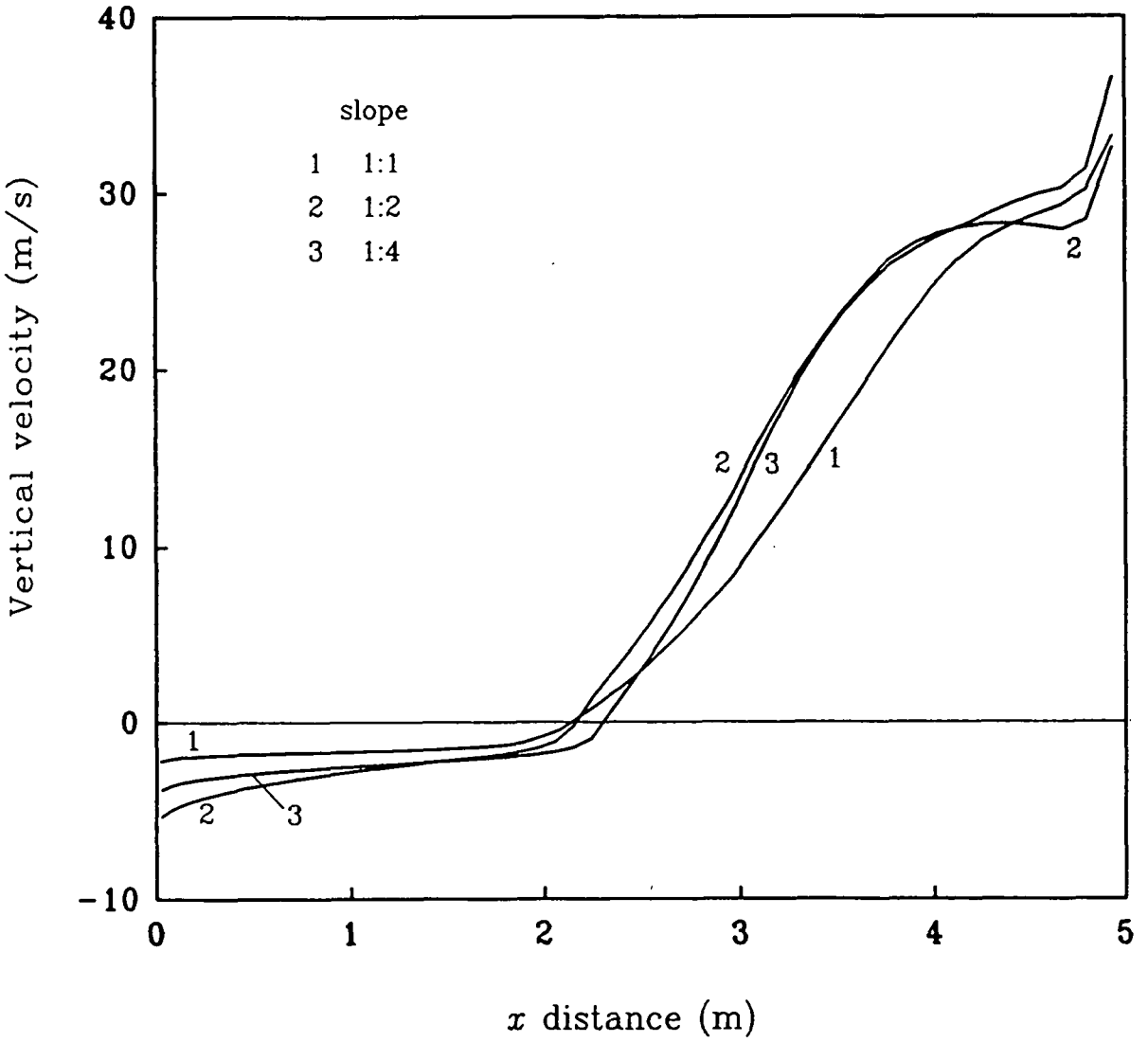

Figure 5. Average vertical velocity distributions at the upper boundaries in the wedge models.

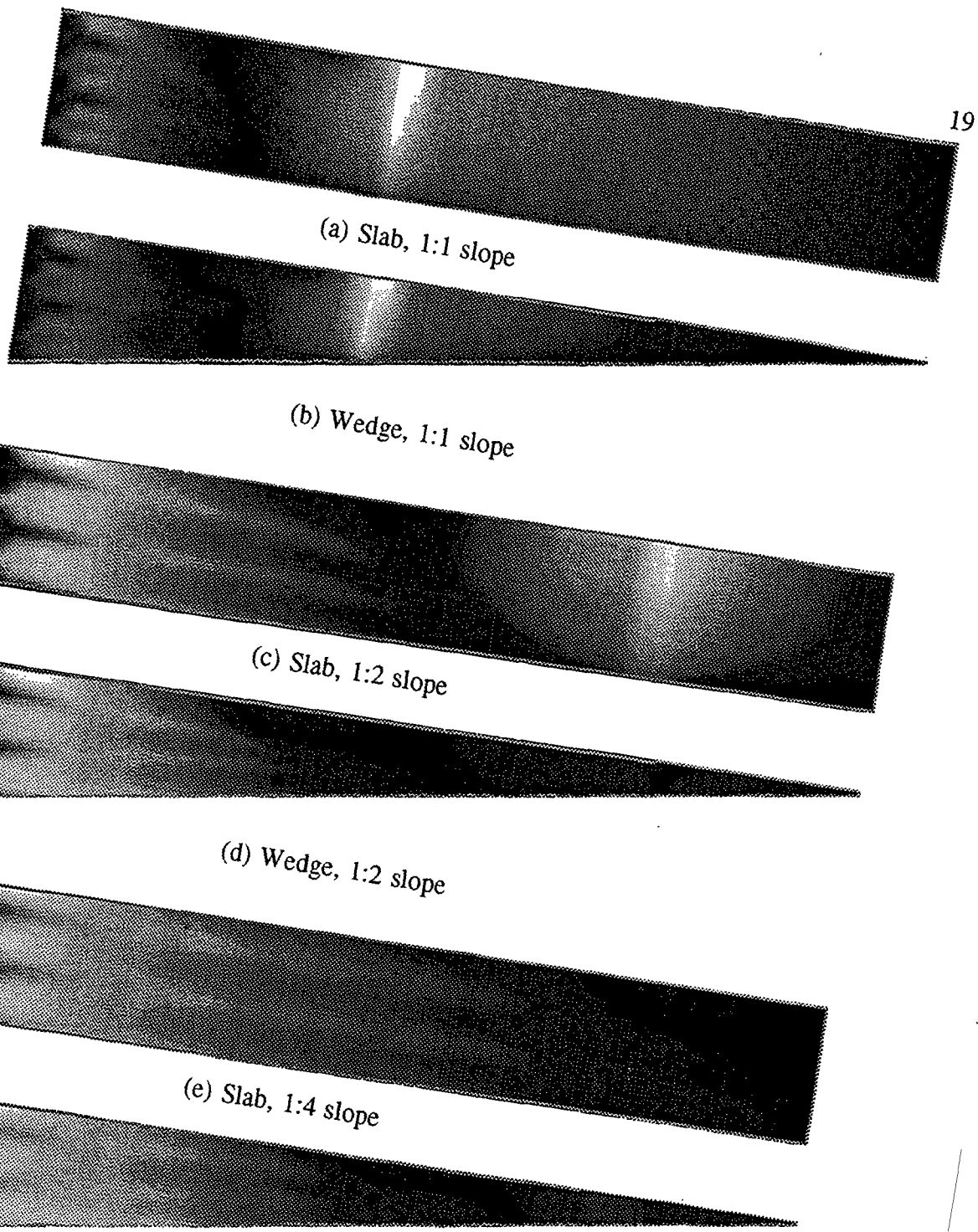

(a) Slab, 1:1 slope

(b) Wedge, 1:1 slope

(c) Slab, 1:2 slope

(d) Wedge, 1:2 slope

(e) Slab, 1:4 slope

(f) Wedge, 1:4 slope

Figure 6. Plan views of shear stress distribution patterns on the char bed surfaces. Gray scale = 0 - 4.04 Pa (dark - bright) for (a) and (b). Gray scale = 0 - 1.45 Pa for (c), (d), (e), and (f).

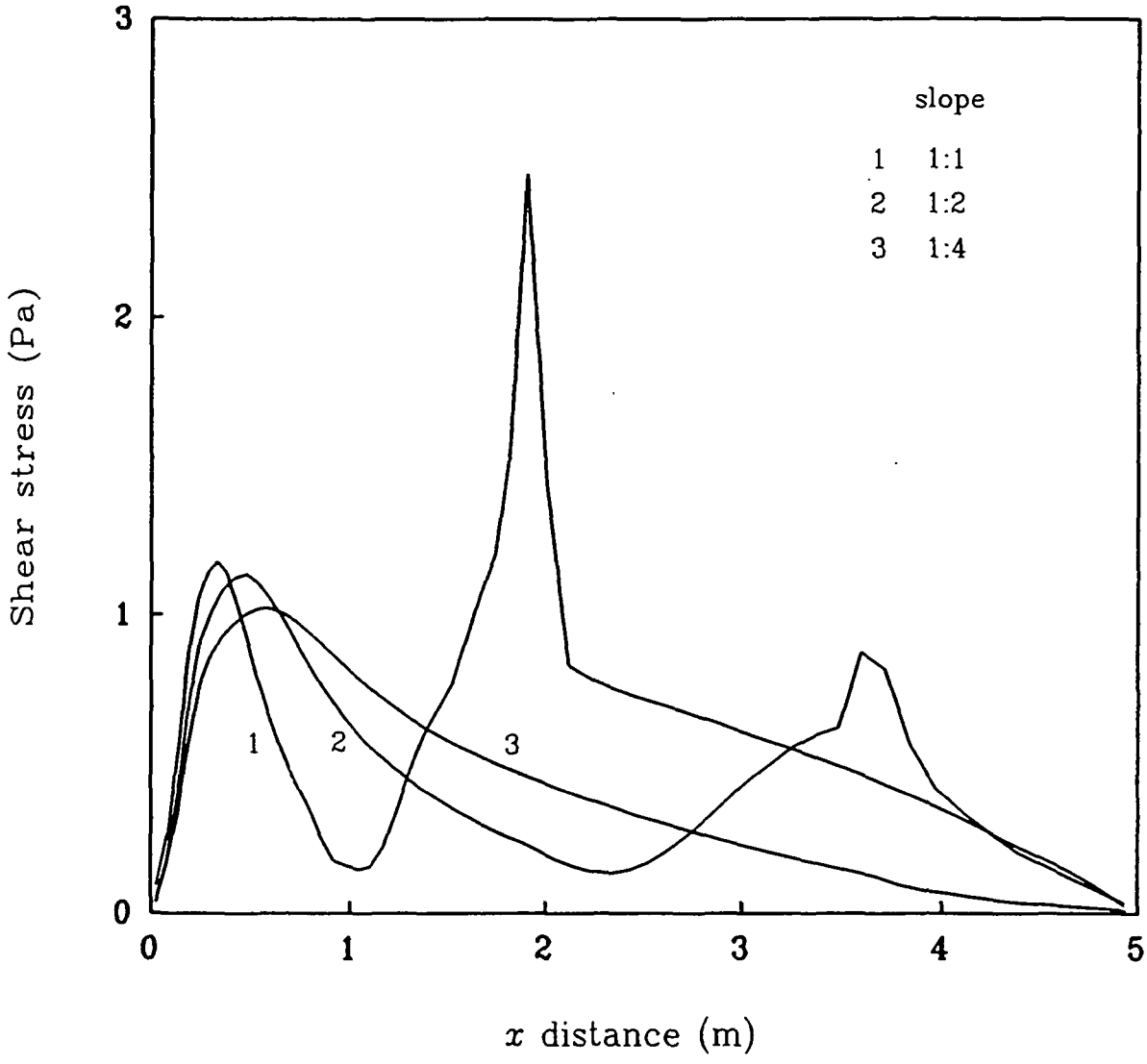

Figure 7. Average shear stress distributions on the char bed surface in the slab models.

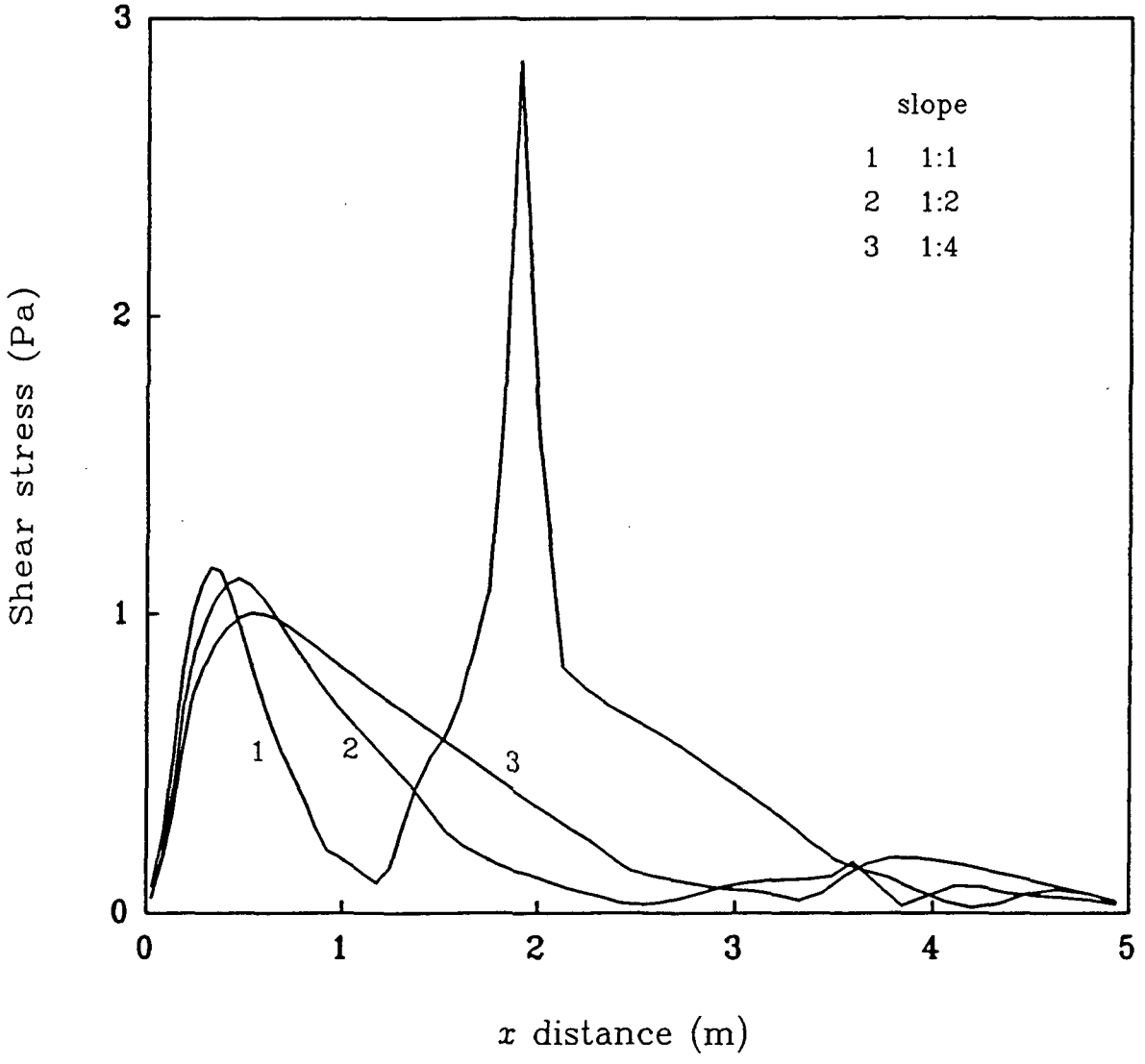

Figure 8. Average shear stress distributions on the char bed surface in the wedge models.

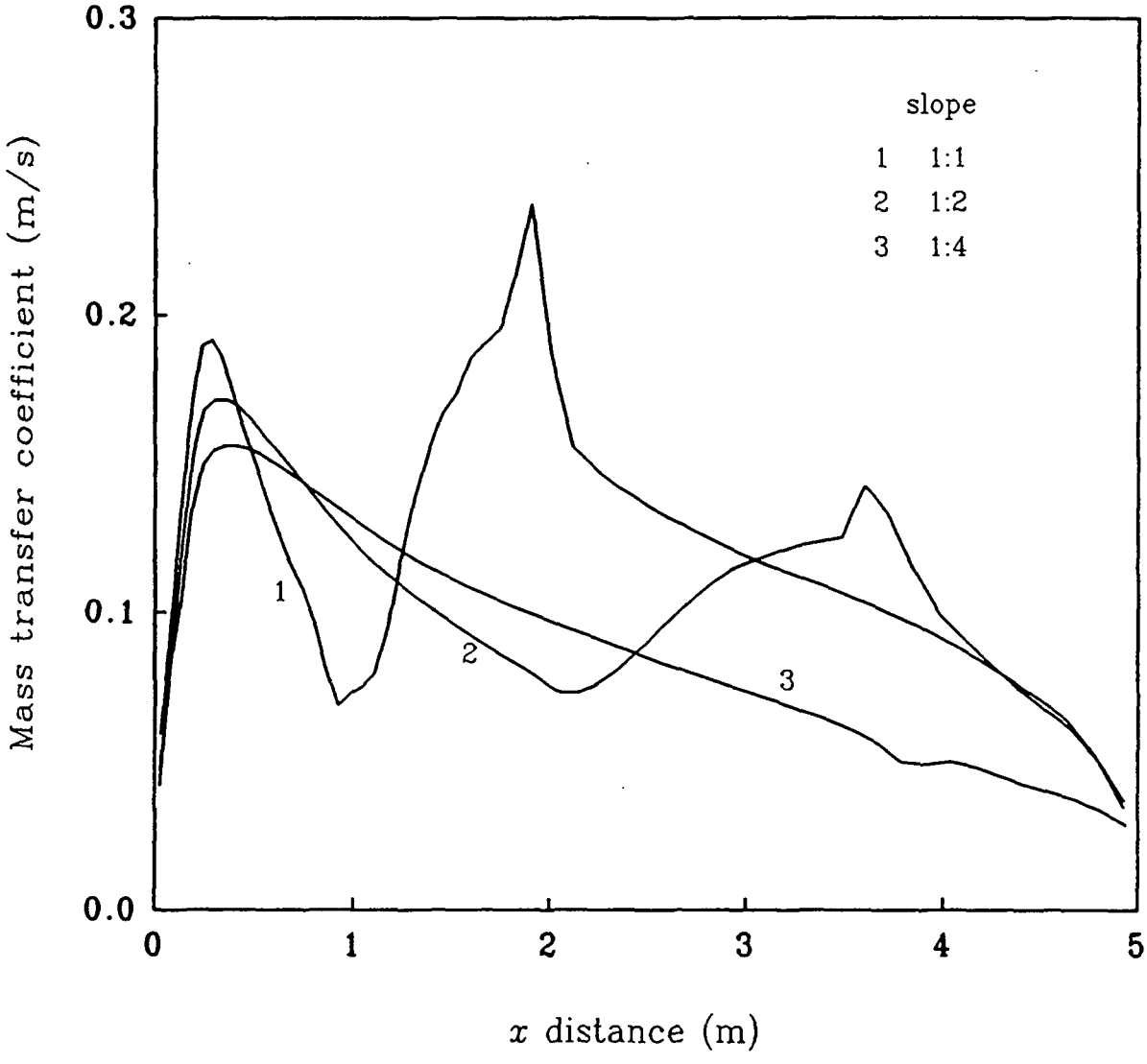

Figure 9. Average mass transfer coefficient distributions on the char bed surface in the slab models.

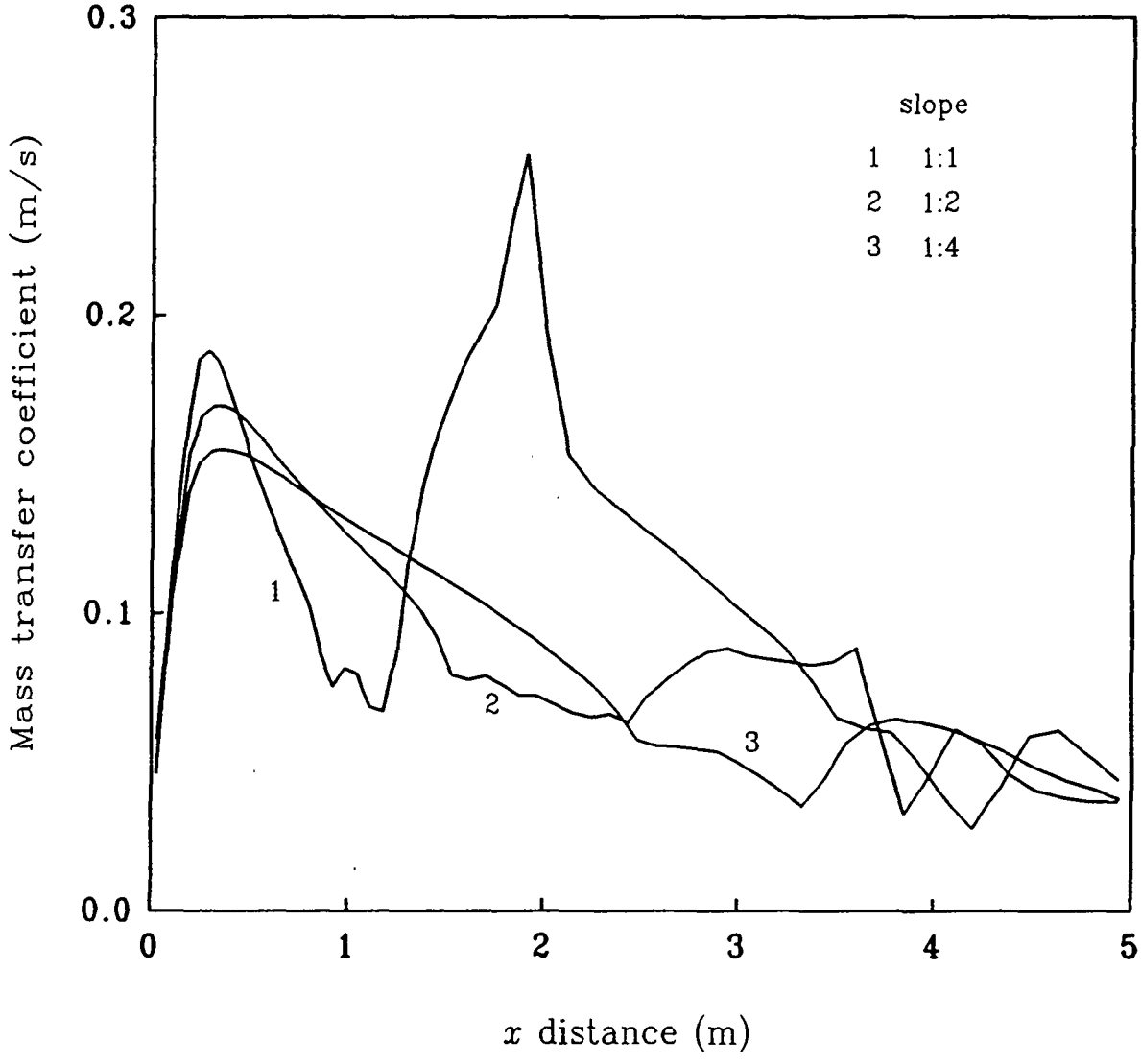

Figure 10. Average mass transfer coefficient distributions on the char bed surface in the wedge models.